Hindawi Publishing Corporation
Advances in Materials Science and Engineering
Volume 2015, Article ID 673025, 10 pages
http://dx.doi.org/10.1155/2015/673025

Research Article

Microstructural Characterization of Beryllium Treated Al-Si Alloys

M. F. Ibrahim,[1] S. A. Alkahtani,[2] Kh. A. Abuhasel,[2] and F. H. Samuel[1]

[1]*Département des Sciences Appliquées, Université du Québec à Chicoutimi, Chicoutimi, QC, Canada G7H 2B1*
[2]*Mechanical Engineering Department, College of Engineering, Prince Sattam bin Abdulaziz University, Al Kharj 11942, Saudi Arabia*

Correspondence should be addressed to F. H. Samuel; fhsamuel@uqac.ca

Received 7 August 2015; Accepted 13 September 2015

Academic Editor: Francesco Delogu

The present study was carried out on B356 and B357 alloys using the thermal analysis technique. Metallographic samples prepared from these castings were examined using optical microscopy and FESEM. Results revealed that beryllium causes partial modification of the eutectic Si, similar to that reported for magnesium additions. Addition of 0.8 wt.% Mg reduces the eutectic temperature by ~10°C. During solidification of alloys containing high levels of Fe and Mg, but no Sr, formation of a Be-Fe phase was detected at 611°C, close to that of α-Al. The Be-Fe phase precipitates in script-like form at or close to the β-Al_5SiFe platelets. A new reaction, composed of fine particles of Si and π-Fe phase, was observed to occur near the end of solidification in high Mg-, high Fe-, and Be-containing alloys. The amount of this reaction decreased with the addition of Sr. Occasionally, Be-containing phase particles were observed as part of the reaction. Addition of Be has a noticeable effect on decreasing the β-Al_5FeSi platelet length; this effect may be enhanced by addition of Sr. Beryllium addition also results in precipitation of the β-Al_5FeSi phase in nodular form, which lowers its harmful effects on the alloy mechanical properties.

1. Introduction

Bäckerud et al. [1] reported that the main reactions to be observed in the Al-7%Si-0.56%Mg alloy containing 0.14 wt.% Fe are (i) the formation of primary α-Al dendrites, (ii) the formation of the Al-Si eutectic phase along with the β-Al_5FeSi phase, and (iii) the formation of secondary eutectic phases. It will be observed that there are two possible reactions required for the formation of the π-phase. The first is a result of the transformation of the β-Al_5FeSi phase into the π-phase through a peritectic reaction. The general microstructure of Al-7%Si-Mg alloys consists of (i) primary α-Al, (ii) Mg_2Si displaying Chinese script morphology, (iii) β-phase (Al_5FeSi) with its plate-like morphology, and (iv) the script-like π-phase ($Al_8Mg_3FeSi_6$) [1].

Phragmén [2] reported that the composition of the β-Al_5FeSi phase is 27 wt.% Fe and 13.5 wt.% Si with a density of 3.30–3.35 g/cm^3, appearing in the form of thin platelets or needles in the microstructure. The β-Al_5FeSi phase grows in a lateral or faceted mode and contains multiple (001) growth twins parallel to the growth direction [3]. The first suggestion of the stoichiometry of the π-phase, from the work of Foss et al. [4], was $Al_9FeMg_3Si_5$, which deviates from the $Al_8Mg_3FeSi_6$ suggested by others [1, 5]. The π-phase is a quaternary phase having a script-like morphology, often linked with β-Al_5FeSi [5]. The chemical composition of the π-phase, observed only in two possible morphologies, is 10.9 wt.% Fe, 32.9 wt.% Si, and 14.1 wt.% Mg, with a density of 2.82 g/cm^3 [5–7].

It has been observed that the addition of strontium acts as an obstacle for the nucleation of the β-Al_5FeSi platelets, by reducing the number of sites ultimately available for nucleation. As a result, the β-Al_5FeSi phase precipitates at a smaller number of sites, leading to the precipitation of needles which are larger compared to those in the nonmodified alloy [8]. It has been reported that for a 319 alloy containing 0.46 wt.% Fe and solidified at a slow cooling rate, the optimum Sr levels lie closer to the limit of 400 ppm: as the Fe level increases, the optimum Sr level will be observed to shift towards the higher limit [9].

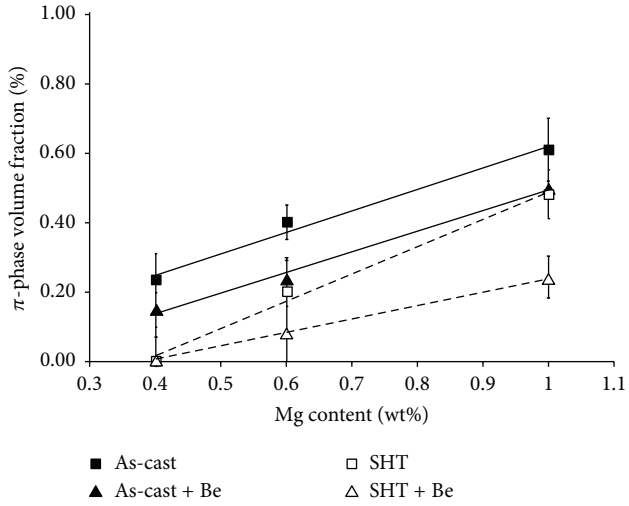

Figure 1: An example of the effect of Be addition on the volume fraction of the π-phase in nonmodified Al-7Si-xMg-0.1Fe Be-containing alloys [5].

For Al-Si-Fe-Mg cast alloys, prior investigations have shown that the amount of π-phase and β-phase may remain constant regardless of the Mg content, whereas the amount of Mg_2Si increases [10]. Cáceres et al. [11] studied the microstructures of two Al-Si-Mg casting alloys, respectively, containing 0.4 wt.% and 0.7 wt.% Mg. It was observed that the iron intermetallic phases in high Mg-content alloys are larger than those are in alloys containing low levels of Mg and that the Fe-rich intermetallic phases in low-Mg alloys were exclusively small β-Al_5FeSi phase plates, while large π-phase ($Al_8Mg_3FeSi_6$) particles were dominant in high-Mg alloys together with a small proportion of the β-Al_5FeSi phase. It has been observed that the addition of Mg to Al-Si-Mg casting alloys, at three different cooling rates, changes the solidification sequence and the type of iron intermetallic phase formed [1]. At Mg additions of more than 1.0 wt.% to molten 319 type alloys, the amount of the β-Al_5FeSi phase is reduced as a result of the transformation of the β-phase into the π-$Al_8Mg_3FeSi_6$ phase [12]. It has been reported that increasing the Mg content from 0.4 to 0.7 wt.% in 357 alloys significantly increases the potential for the formation of the Mg-containing $Al_8FeMg_3Si_6$ iron intermetallic phase [13].

The present study is an extension of the work carried by Elsharkawi, Figure 1 [5], on the effects of metallurgical parameters on the decomposition of the π-$Al_8Mg_3FeSi_6$ phase in Al-Si-Mg alloys, with an emphasis on the role of Be, Sr in the microstructural features of B356 and B357 alloys, by first considering the role of increasing both the Mg and Fe content.

2. Experimental Procedure

Both B356 and B357 alloys were investigated in the present study. The Mg level was increased by adding pure Mg to the alloy melts to obtain Mg levels of 0.4 wt.%, 0.6 wt.%, and 0.8 wt.%. The Fe and Be were added in the form of Al-25 wt.% Fe and Al-5 wt.% Be master alloys, respectively, to the alloy melt to obtain Fe levels of 0.09 wt.%, 0.2 wt.%, and 0.6 wt.% and a Be level of 0.05 wt.%. Sr (0.02 wt.%) and Ti (0.15 wt.%) were added to the alloy melts in the form of Al-10%Sr and Al-5 wt.% Ti-1 wt.% B master alloys, for Sr-modification and grain refining purposes, respectively. Table 1 presents the chemical composition of the alloys used in the present study.

Table 1: Average chemical composition (wt%) of the 356 and 357 alloys studied.

Alloy code	Element concentration (wt%)						
	Si	Fe	Mg	Ti	Sr	Be	Al
A1	7.146	0.09	0.40	0.168	0.00	0.00	Bal.
A1B	7.146	0.09	0.40	0.168	0.00	0.05	Bal.
A1S	7.146	0.09	0.40	0.168	0.02	0.00	Bal.
A1BS	7.146	0.09	0.40	0.168	0.02	0.05	Bal.
C3	7.146	0.60	0.80	0.168	0.00	0.00	Bal.
C3B	7.146	0.60	0.80	0.168	0.00	0.05	Bal.
C3S	7.146	0.60	0.80	0.168	0.02	0.00	Bal.
C3BS	7.146	0.60	0.80	0.168	0.02	0.05	Bal.

In the above table, codes A and C correspond to the Fe levels 0.09 and 0.6, respectively, while codes 1, 2, and 3 correspond to the Mg levels 0.4, 0.6, and 0.8, respectively. B and S represent Be and Sr, respectively.

Thermal analysis is used to examine the combined interaction between strontium and boron, as well as the likely effect of boron in partial modification of the eutectic Si particles. Near equilibrium conditions (i.e., very slow cooling rate) were achieved through the use of a graphite cup preheated to 600°C. Approximately 600 grams of the alloy was taken in a SiC crucible and was poured at 735°C ± 5°C (100°C above the liquidus). The temperature was measured by K-type (chromel-alumel) thermocouples located at the centerline position within the sample cup at midheight. Cooling curves were recorded and the castings were sectioned perpendicular to the axis of the cylinder, at the level of the thermocouple, and then polished/etched for metallographic purposes.

The dendrite arm spacing (DAS) values were determined from metallography samples using Climax image analyzer system in conjunction with optical microscope. At least 40 measurements were made for each sample and the average value of at least 100 dendrites was taken to represent the DAS value for the corresponding level.

A quantitative evaluation of the eutectic Si particle characteristics was carried out using image analysis. From these measurements, the average value and standard deviation were obtained in each case. Samples for metallography were examined using optical microscopy as well as scanning electron microscopy (SEM), coupled with energy dispersive X-ray spectrometry (EDS), and wavelength dispersion spectrometry (WDS) detectors.

3. Results and Discussion

3.1. Si Particles. The silicon particle characteristics for the various alloy compositions investigated are summarized in Table 2, in which the Si particle measurements for the A1 base alloy samples, with low Mg and low Fe content using

Table 2: Silicon particle measurements for the as-cast 357 alloy samples (obtained from graphite mold castings, DAS 65 μm).

Alloy (condition)	Area (μm^2)		Length (μm)		Roundness ratio (%)		Aspect ratio	
	Av.	SD	Av.	SD	Av.	SD	Av.	SD
A1 (nonmod.)	76.70	71.50	21.60	16.30	28.4	21.8	3.52	4.54
C3 (nonmod.)	20.70	22.70	9.63	7.98	36.2	21.4	2.86	5.84
A1B (Be mod.)	49.60	52.40	15.20	12.00	33.8	21.8	2.85	3.45
C3B (Be mod.)	13.60	14.30	6.75	5.08	43.7	22.2	2.27	1.15
A1S (Sr mod.)	3.18	3.21	3.05	2.16	46.0	19.2	2.11	2.14
C3S (Sr mod.)	4.48	4.78	3.82	3.07	43.4	21.5	2.46	3.87
A1BS (Be + Sr mod.)	2.75	2.94	3.00	2.38	43.5	19.5	2.18	2.25
C3BS (Be + Sr mod.)	3.38	3.97	3.27	2.69	43.9	19.8	2.15	1.32

the graphite mold giving a DAS of ~65 μm, are listed. It can be seen that the Si particle area decreased from 76.70 to 3.18 μm^2, the Si particle length decreased from 21.60 to 3.05 μm, and the aspect ratio decreased from 3.52 to 2.11, while the roundness ratio increased from 28.4 to 46.0% after Sr-modification in the alloy A1S sample. In the case of Be addition (alloy A1B), the Si particle area decreased to 49.60 μm^2, the Si particle length decreased to 15.20 μm, and the aspect ratio decreased to 2.85, while the roundness ratio increased to 33.8%. The presence of both Sr and Be in alloy A1BS resulted in decreasing the Si particle area to 2.75 μm^2, decreasing the Si particle length to 3.0 μm, decreasing the aspect ratio to 2.18, and increasing the roundness ratio to 43.5%. After increasing the Mg and Fe contents (alloy C3), the Si particle area decreased to 20.7 μm^2, the Si particle length decreased to 9.63 μm, and the aspect ratio decreased to 2.86, while the roundness ratio increased to 36.2%. The combined effect of the four elements (alloy C3BS) resulted in decreasing the Si particle area to 3.38 μm^2, decreasing the Si particle length to 3.27 μm, decreasing the aspect ratio to 2.15, and increasing the roundness ratio to 43.9%. The values listed reflect the modification effect of Sr and partial modification effects of Mg and Be, but with increasing Fe levels it appears that most of the Be reacts with the Fe to form a Be-Fe phase (most probably, Al_8Fe_2BeSi [14]), thereby reducing the partial modification effect attributed to Be.

3.2. Thermal Analysis

3.2.1. Effects of Iron and Magnesium Content. Thermal analysis was carried out to determine the precipitation sequence and formation temperature of the intermetallic phases observed in the 357 alloys containing different levels of Fe and Mg. In this respect, alloys A1, C3BS, and C3B were selected as examples. The reactions and corresponding temperatures observed in the cooling curves for the alloys studied are summarized in Table 3. Figure 2(a) represents solidification of the base alloy A1, showing the precipitation of α-Al (1), followed by formation of the Al-Si eutectic phase (2), together with the precipitation of the β-Al_5FeSi. It is expected that as solidification proceeds, the β-phase content present will be transformed into the π-phase as a result of the preeutectic reaction (3), $L + Al_5FeSi \rightarrow Al + Si + Al_8Mg_3FeSi_6$. The last reaction (4) is characterized by a wide peak, which may arise from two merged reactions; first reaction is related to the formation of Mg_2Si followed by the second reaction which corresponds to the quaternary reaction, $L \rightarrow Al + Si + Mg_2Si + Al_8Mg_3FeSi_6$.

By comparing the first derivative curve in Figure 2(a) with the one shown in Figure 3(a) for alloys A1 (base alloy) and C3BS, respectively, it will be seen that, at 0.09 wt.% Fe, for the A1 base alloy, the first derivative curve reveals four peaks, while at 0.6 wt.% Fe, C3BS alloy, a new peak marked (2) may be observed before the eutectic reaction. This peak corresponds to the formation of the preeutectic β-phase, while the precipitation of Mg_2Si was formed with reaction (4). Reaction (5) may be explained as

$$L + Al_5FeSi \longrightarrow Al + Si + Al_8Mg_3FeSi_6 \quad (1)$$

where β-Al_5FeSi phase was transformed into the π-phase. Other reactions remain the same as those described in Figure 4(a).

To reach a better understanding of the effect of Fe content on intermetallic formation, it has been reported [15, 16] that increasing the Fe content from 0.09 wt.% to 0.6 wt.% changes the solidification sequences of Al-7Si-0.4Mg alloys (base alloy A1), which can be explained by the current thermal analysis. At 0.09 wt.% Fe, the β-phase precipitates at low temperatures together with the Al-Si eutectic phase and is characterized by fine platelets in the microstructure, as shown in Figure 2(b). At 0.6 wt.% Fe, most of the β-phase will precipitate at high temperatures before the Al-Si eutectic phase. This β-phase is characterized by much larger size in the microstructure, as shown in Figures 3(b) and 3(c). As a result, increasing the Fe content will increase the size of the β-phase in the microstructure, which would have a negative effect on the alloy mechanical properties.

For a clear understanding of the effects of Mg addition on the precipitation sequence and reaction temperature, the Mg content in Sr-modified alloy C3BS (Figure 5), also in non-modified alloy C3B (Figure 4), was increased up to 0.8 wt.%. Two separate peaks were identified corresponding to reactions (4) and (5). The reactions and their corresponding formation temperatures during solidification of alloys C3BS and A1, containing high and low Mg levels, respectively, are listed in Table 3. There is a significant reduction in the eutectic temperature by ~10°C in high Mg-containing alloy (C3BS),

Table 3: Main reactions observed from thermal analysis data of alloys A1, C3BS, and C3B.

Alloy code	Temp. (°C)	Reaction [21]
A1 0.09%Fe-0.4%Mg	612 (1)	Formation of Al-dendritic network
	569 (2)	(i) Precipitation of Al-Si-eutectic phase (ii) Precipitation of posteutectic β-Al_5FeSi phase
	561 (3)	Transformation of β-phase into π-$Al_8Mg_3FeSi_6$ phase
	546 (4)	(i) Precipitation of Mg_2Si (ii) Quaternary eutectic reaction*
C3BS 0.6%Fe-0.8%Mg-0.05%Be-0.02%Sr	609 (1)	Formation of Al-dendritic network
	568 (2)	Formation of preeutectic β-Al_5FeSi phase
	561 (3)	(i) Precipitation of Al-Si-eutectic phase (ii) Precipitation of posteutectic β-Al_5FeSi phase
	550 (4)	(i) Transformation of β-phase into π-$Al_8Mg_3FeSi_6$ phase (ii) Precipitation of Mg_2Si
	540 (5)	Quaternary reaction*
C3B 0.6%Fe-0.8%Mg-0.05%Be	613 (1)	Formation of Al-dendritic network
	611 (2)	Formation of Be-Fe phase
	560 (3)	(i) Precipitation of Al-Si-eutectic phase (ii) Precipitation of posteutectic β-Al_5FeSi phase
	551 (4)	(i) Transformation of β-phase into π-$Al_8Mg_3FeSi_6$ phase (ii) Precipitation of Mg_2Si
	539 (5)	Quaternary reaction*

*Quaternary reaction, $L \rightarrow Al + Si + Mg_2Si + Al_8Mg_3FeSi_6$.

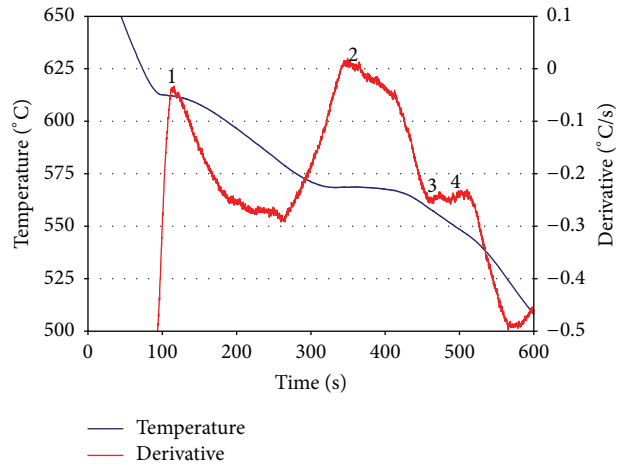

(a)

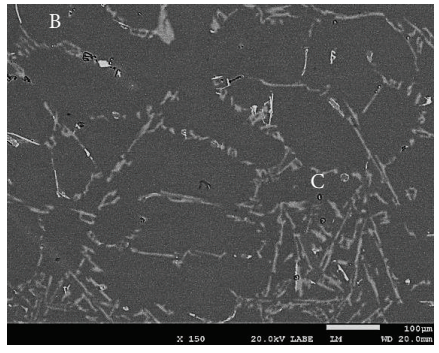

(b)

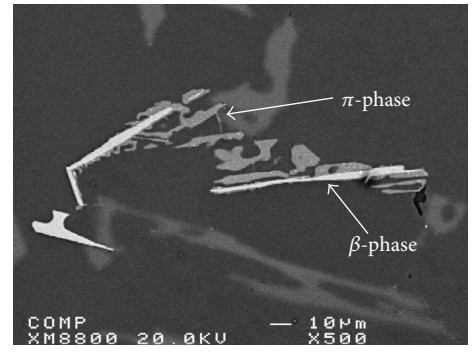

(c)

Figure 2: (a) Temperature-time cooling curve and its first derivative obtained from the base alloy A1, (b) the corresponding microstructure showing small size of the β-Al_5FeSi phase and the π-$Al_8Mg_3FeSi_6$ phase particles, and (c) partial transformation of β-Al_5FeSi to π-phase.

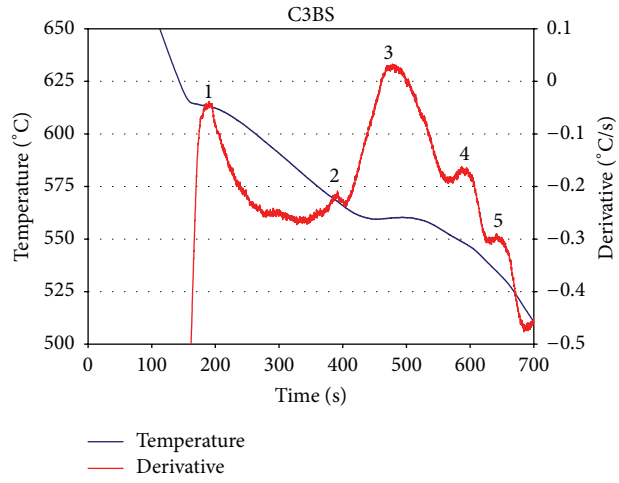

(a)

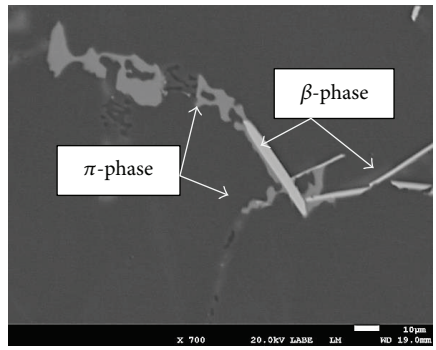

(b)

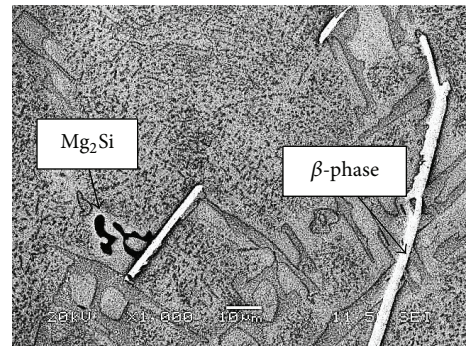

(c)

FIGURE 3: (a) Temperature-time cooling curve and its first derivative obtained from the alloy C3BS, (b) the corresponding microstructure showing much bigger size of the β-Al_5FeSi phase and the π-phase particles, and (c) the corresponding microstructure showing much larger size of the β-phase and the Mg_2Si particles.

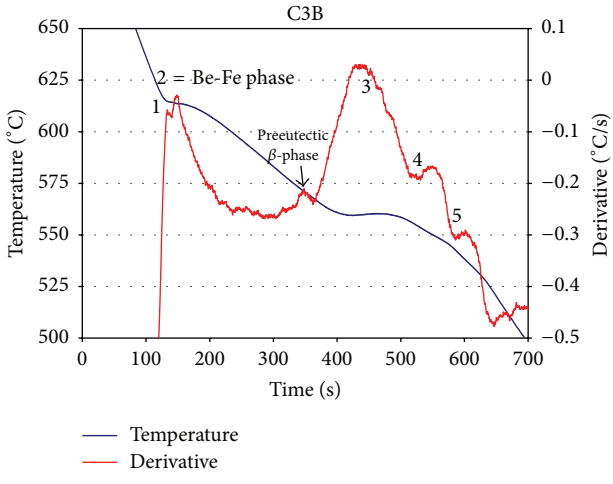

(a)

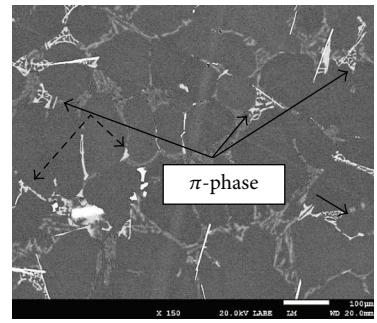

(b)

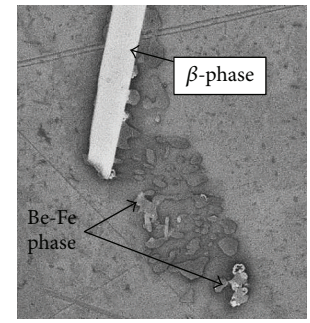

(c)

FIGURE 4: (a) Temperature-time cooling curve and its first derivative obtained from the nonmodified alloy C3B, (b) the corresponding microstructure showing a noticeable larger size of the nodular β-Al_5FeSi phase (broken arrows) and the π-$Al_8Mg_3FeSi_6$ phase particles, and (c) enlarged microstructure showing small particles possibly Be-Fe phase and/or π-phase particles close to β-phase plate-black arrows.

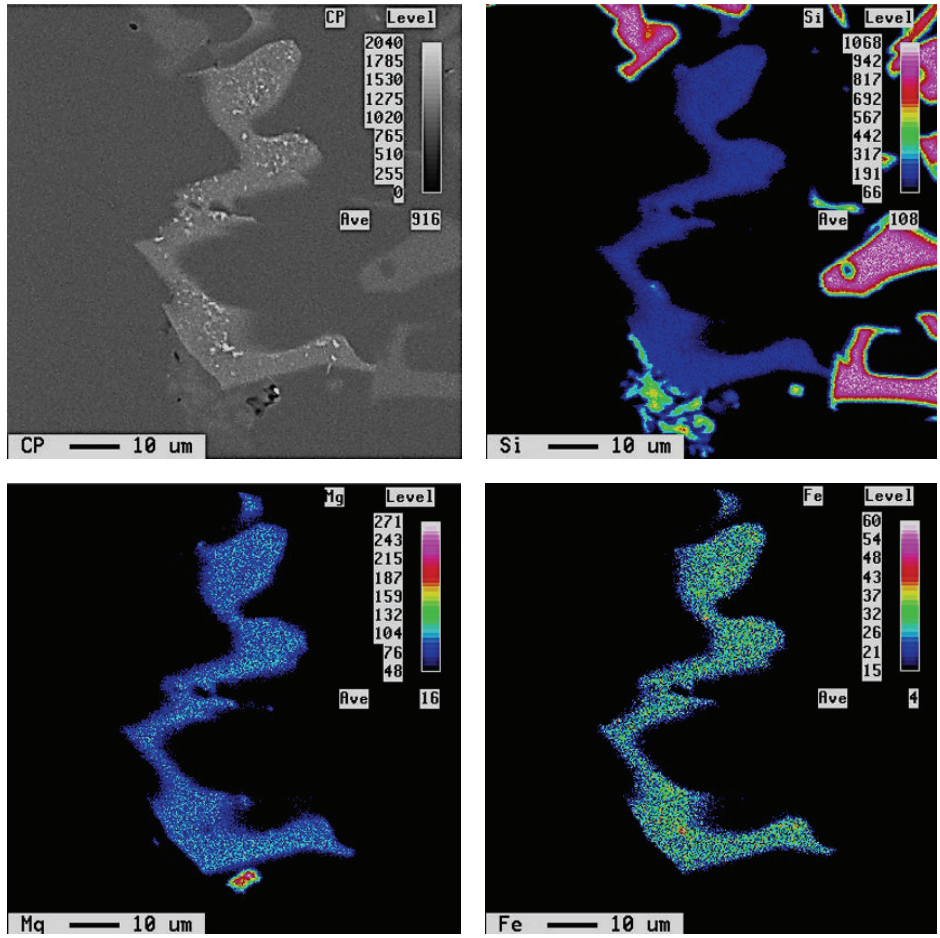

Figure 5: Element distribution in π-phase.

compared to the low Mg-containing alloy (A1), which is in a good agreement with published findings [17]. Moustafa et al. [18] reported that the observed reduction in eutectic temperature affects the modification of the eutectic Si particles.

After an extensive investigation of the microstructure, the π-$Al_8Mg_3FeSi_6$ phase is often observed to be in close contact with β-Al_5FeSi phase platelets. Figure 2(c) is an enlarged micrograph revealing the transformation of the β-phase to π-phase. Thus it may be reasonable to assume that the β-Al_5FeSi phase will precipitate first followed by the growth of the π-$Al_8Mg_3FeSi_6$ phase from the surface of the β-Al_5FeSi thereafter, according to

$$L + Al_5FeSi \longrightarrow Al + Si + Al_8Mg_3FeSi_6 \quad (2)$$

Figure 7 shows the elements distribution in the π-phase.

3.2.2. Effects of Beryllium Content. The morphology of iron intermetallic shows the precipitation of several types in Be-containing and Be-free alloys. The Fe intermetallics observed in the optical microstructure of the Al-7Si-0.8Mg-0.6Fe-0.05Be, C3B alloy, are (i) the nodular Fe-Si-Al β-phase and (ii) Be-Fe phase (Al_8Fe_2BeSi) with a script-like morphology, as presented in Figures 3(b) and 3(c). This observation is in agreement with the reported microstructure of Be-containing B357 alloys [19, 20]. It is shown in Figures 5 and 6 that the Be-Fe phase exists near or at the β-phase platelets. A similar observation can be made from the thermal analysis results of the C3BS alloy. It is estimated that the formation temperature of this reaction is approximately 611°C which is close to the formation temperature of α-AL; this would facilitate the precipitation of the Be-Fe phase in the interdendritic region, within the α-AL, or both, especially in high Be-containing alloys of the order of 0.2 wt.% [14, 20–23]. Also, this temperature is higher than the formation temperature of the preeutectic β-Al_5FeSi phase marked as peak (2) in Table 3 for the Be-free A1 alloy and for the Sr-modified Be-containing C3BS alloy, as shown in Figures 2 and 4.

Based on the thermal analysis data and the corresponding microstructure, the addition of Be resulted in a change in the precipitation sequence of the iron intermetallics where peak (2) (Figure 6(a)) corresponds to the possible formation of the Be-Fe phase. This observation was supported by Murali et al. [20–22], who carried out an interrupted quenching experiment to detect the formation temperature of the Be-Fe phase (Al_8Fe_2BeSi). The authors found that the Be-Fe phase exists in the microstructure at the point where the melt quenched from the liquid temperature at 607°C. However, in the present work, the exact composition of the Be-Fe

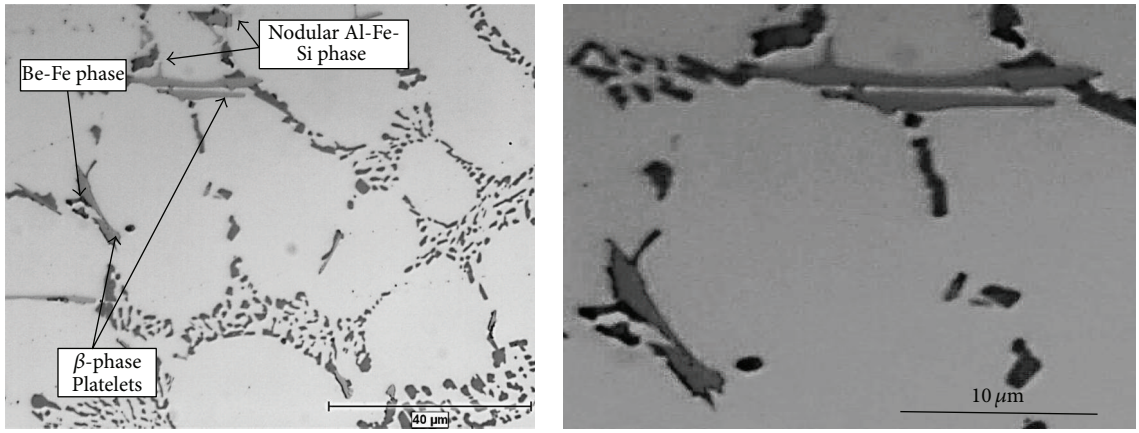

(a) (b)

Figure 6: Optical microstructures of Sr-modified C3BS alloy showing (a) nodular and platelet forms of Al_5FeSi, β-phase, and π-phase particles and possibly Be-Fe containing phase particles. (b) Enlarged portion of (a) revealing the irregular shape of the β-Al_5FeSi platelets.

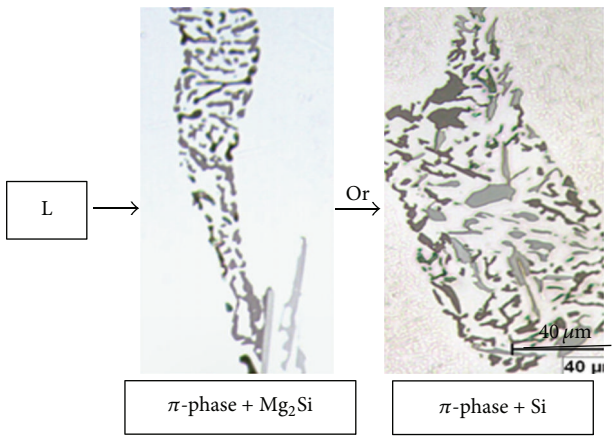

Figure 7: Optical microstructures of Be-containing C3B alloy showing the new eutectic-like reaction sequence.

phase could not be identified with certainty. The precipitation sequence and the corresponding temperatures for the Al-7Si-0.8Mg-0.6Fe Be-containing alloy, in both the nonmodified and Sr-modified conditions C3B and C3BS, are listed in Table 3. Figure 8(a) is an optical microstructure of the Sr-modified C3BS Be-containing alloy showing nodular Al-Fe-Si, in addition to other phases, whereas Figure 6(b) reveals the irregular shape of the β-phase platelets that may be caused by the addition of Be and its reaction with Fe.

3.3. Observation of a New Reaction. Figure 3 displays the cooling curve and its first derivative obtained from the C3BS alloy. From an examination of the microstructure of both the nonmodified and Sr-modified, Be-containing alloys, particularly alloys containing higher levels of Mg and Fe (alloys C3B and C3BS), a new reaction was observed to take place towards the end of solidification at a low cooling rate (0.4°C/s), as shown in Figure 7. This new reaction is composed of a mixture of Mg_2Si, π-$Al_8Mg_3FeSi_6$ phase, Si particles, and possibly Be-Fe phase. It should be mentioned here that this reaction was not detected in any of the cooling curves, since the heat associated with this reaction is apparently too low. Table 4 lists the solidification times obtained from the C3 series of alloys. As can be seen, the solidification time for the C3B alloy is ~22 seconds more than that obtained from the C3 base alloy. It may be suggested that this increase in the solidification time, due to the presence of Be, would result in the decomposition of the remaining liquid metal into the newly observed reaction [24]. However, the exact mechanism by which this reaction took place requires more investigation.

Table 4: Solidification times of the A and C3 series of alloys obtained from their cooling curves. Each value is an average of five consecutive tests.

Alloy code	Solidification time (s)
A1	452
A1B	464
A1S	472
A1BS	474
C3	463
C3B	492
C3S	510
C3BS	504

Beryllium and strontium are the main parameters controlling the amount of this new reaction or precipitates. Table 5 summarizes the area and intensity measurements of the new reaction. It is found that addition of Sr to the nonmodified, Be-containing C3B alloy decreased the reaction particle area by 44% and intensity by 36%, respectively. Figure 8 is an example of the element distribution within the new reaction.

The intermetallic phases present in the alloys studied were of two types: either completely soluble or partially soluble. The Mg_2Si phase was the completely soluble one as observed in the cast structure. This phase appears darker than, or closer

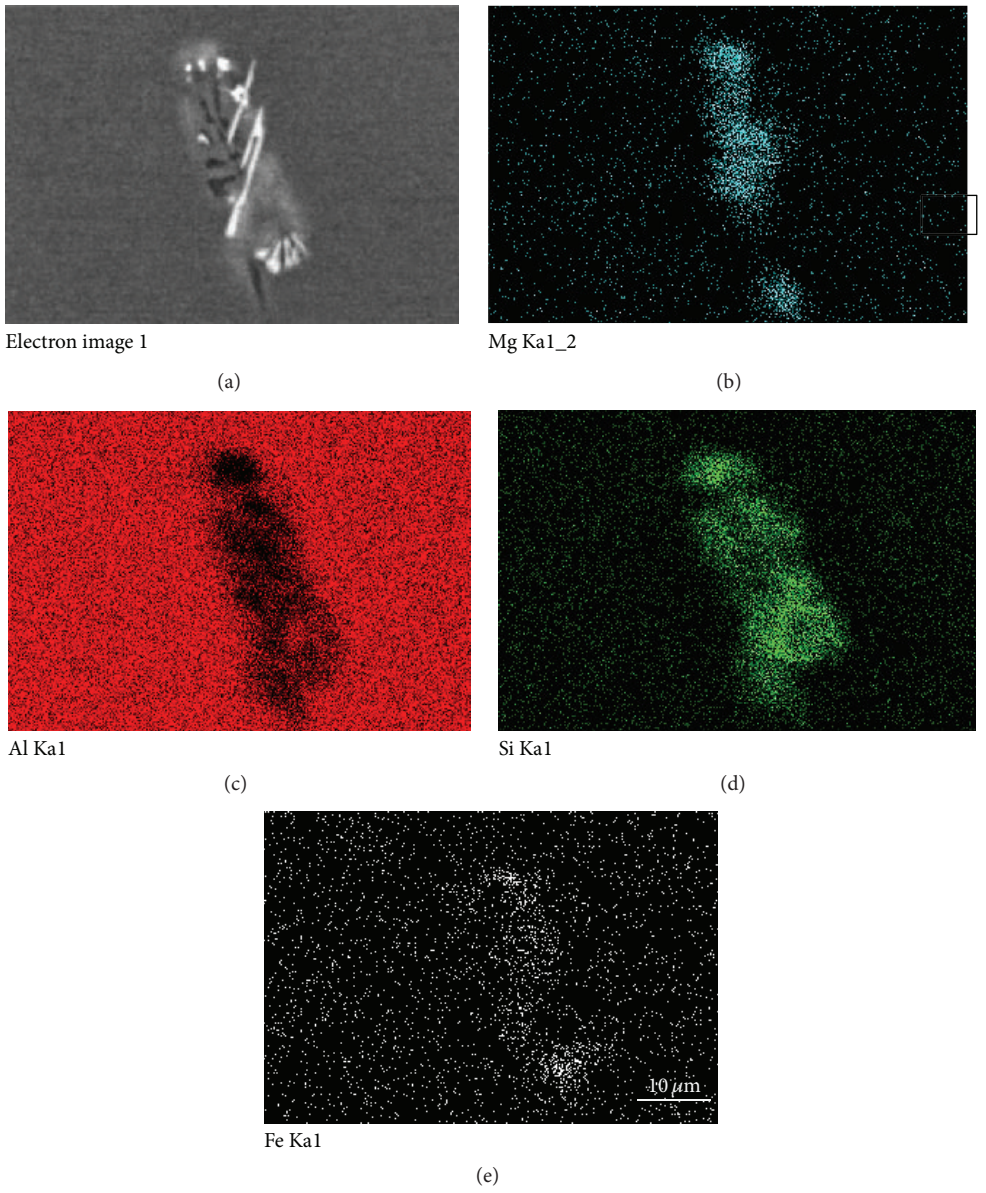

Figure 8: (a) Backscattered image, and images of (b) Mg, (c) Al, (d) Si, and (e) Fe distribution within the new eutectic reaction.

Table 5: New reaction particle measurements for the as-cast 357 alloys.

Alloy code	Area (%)		Area (μm^2)		Intensity (particle/field)
	Av.	SD	Av.	SD	
C3B	5.87	2.46	1155.2	1242.0	17.34
C3BS	3.30	1.64	662.8	805.5	11.22

to, the degree of darkness in the backscattered images of the Al-matrix because of their smaller average atomic number. The Mg_2Si phase dissolves during the solutionizing treatment where Mg diffuses into the metal matrix and forms a supersaturated solid solution after quenching. The principal partially soluble phases in the B357 casting alloys are the β-Al_5FeSi and π-$Al_8Mg_3FeSi_6$ compounds, as well as the Be-Fe phase.

An intensive study [5] was carried out on the decomposition of the π-$Al_8Mg_3FeSi_6$ phase in an Al-Si-Mg B357-type alloy. This study has addressed this subject in detail, in which the reason leads to concentrating on investigating the characteristics of β-Al_5FeSi phase as the most iron intermetallic phase has a negative effect on the mechanical properties of such casting alloys, where this study has concluded that, after the recommended solution treatment, the Chinese-script π-$Al_8Mg_3FeSi_6$ phase is completely decomposed into fine needles of the β-Al_5FeSi phase at 0.4 wt.% Mg but appears to only be partially decomposed at higher Mg contents, namely, 0.6–0.8 wt.%. The second conclusion reported was that adding of 500 ppm of Be reduces the amount of the π-phase formed in Al7SixMg-0.1Fe alloys; such Be additions also facilitate the decomposition of the π-phase into the β-Al_5FeSi phase, particularly at higher levels of Mg content.

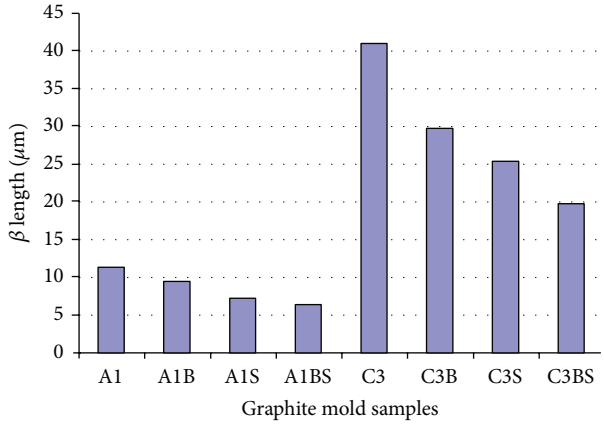

FIGURE 9: Histogram exhibiting the variation in β-Al_5FeSi phase average length affected by the composition of the alloys.

Another conclusion suggested that long solutionizing times lead to a significant reduction in the amount of the π-phase through the dissolution and decomposition of the π-phase into fine β-Al_5FeSi phase platelets.

The histogram in Figure 9 illustrates the effects of Fe, Mg, Be, and Sr additions on the length of the β-Al_5FeSi phase. It is reported that iron intermetallics are affected by the cooling rate. Thus increasing cooling rate from using a graphite mold (DAS~65 μm) to a metallic mold (DAS~24 μm) would lead to decreasing the length of the β-Al_5FeSi phase by ~50%. Also, a similar reduction in the β-phase length can be obtained by adding Be and/or Sr. Increasing Mg and Fe up to 0.6 and 0.8 wt.%, respectively, results in a similar effect of reducing the β-phase length. Additionally, increasing both of these elements increases the amount of the π-phase in the matrix. These results agree with the work of Elsharkawi [5].

Figure 9 also illustrates how the addition of 0.02 wt.% Sr to Al-7Si-Mg-Fe alloys results in a slight decrease in the β-phase length, or the amount of the β-phase, when compared to nonmodified alloys. This may be explained in terms of the presence of Sr which results in the breaking up of the β-phase platelets, as reported by Samuel et al. [25], thereby reducing the length and increasing the density of this β-Al_5FeSi phase platelets. The authors claim that Sr was absorbed by the β-Al_5FeSi phase platelets leading to their destabilization and fragmentation. This observation may contribute to an increase in the number of β-Al_5FeSi platelets available for the preeutectic reaction to occur, thereby forming further amounts of the π-$Al_8Mg_3FeSi_6$ phase.

4. Conclusions

Based on the microstructural results obtained from applying thermal analysis, the following conclusions may be drawn:

(1) Beryllium brought about partial modification of eutectic Si particles, for example, 76.7 μm^2 versus 49.60 μm^2, respectively.

(2) Addition of 0.8 wt.% Mg reduced the eutectic temperature by ~10°C.

(3) During solidification of alloys containing high levels of Fe and Mg (but no Sr), a peak corresponding to the formation of the Be-Fe phase (most probably Al_8Fe_2BeSi) was observed; however the exact composition could not be identified with certainty.

(4) The Be-Fe phase precipitates in the form of a script-like morphology at or close to β-platelets.

(5) A new reaction was observed to take place near the end of solidification of high Mg-, high Fe-, and Be-containing alloys. This new reaction is composed mainly of fine particles of Si and π-$Al_8Mg_3FeSi_6$ phases.

(6) Addition of Be has a noticeable effect on decreasing the β-Al_5FeSi phase length. This effect may be enhanced by the addition of Sr.

Conflict of Interests

The authors declare that there is no conflict of interests regarding the publication of this paper.

Acknowledgments

Financial and in-kind support received from the Natural Sciences and Engineering Research Council of Canada is appreciated. The authors would to thank Ms. Amal Samuel for enhancing the quality of the artwork presented in this paper.

References

[1] S. L. Bäckerud, G. Chai, and J. Tamminen, *Solidification Characteristics of Aluminum Alloys Vol 2: Foundry Alloys*, AFS/Skanaluminium, Oslo, Norway, 1990.

[2] G. Phragmén, "On the phases occurring in alloys of aluminum with copper, magnesium, manganese, iron, and silicon," *Journal of the Institute of Metals*, vol. 77, pp. 498–553, 1950.

[3] S. K. Tang and T. Sritharan, "Morphology of β-AlFeSi intermetallic in Al-7Si alloy castings," *Materials Science and Technology*, vol. 14, no. 8, pp. 738–742, 1998.

[4] S. Foss, A. Olsen, C. J. Simensen, and J. Taftø, "Determination of the crystal structure of the π-AlFeMgSi phase using symmetry- and site-sensitive electron microscope techniques," *Acta Crystallographica—Section B: Structural Science*, vol. 59, no. 1, pp. 36–42, 2003.

[5] E. A. Elsharkawi, *Effect of metallurgical parameters on the decomposition of the π-AlFeMgSi phase in Al-Si-Mg alloys and its influence on the mechanical properties [Ph.D. thesis]*, Université du Québec à Chicoutimi, Chicoutimi, Canada, 2011.

[6] L. F. Mondolfo, *Aluminum Alloys: Structure and Properties*, Butterworths, London, UK, 1976.

[7] J. A. Taylor, "The effect of iron in the Al-Si casting alloys," in *Proceedings of the 35th Australian Foundry Institute National Conference on Casting Concepts*, Adelaide, Australia, October 2004.

[8] A. M. Samuel, F. H. Samuel, and H. W. Doty, "Observations on the formation of β-Al_5FeSi phase in 319 type Al-Si alloys," *Journal of Materials Science*, vol. 31, no. 20, pp. 5529–5539, 1996.

[9] A. Pennors, A. M. Samuel, F. H. Samuel, and H. W. Doty, "Precipitation of β-Al_5FeSi iron intermetallic in Al-6Si-3.5Cu

(319) type alloys: role of Sr and P," *AFS Transactions*, vol. 106, pp. 251–264, 1998.

[10] J. A. Taylor, D. H. StJohn, L. H. Zheng, G. A. Edwards, J. Barresi, and M. J. Couper, "Solution treatment effects in Al-Si-Mg casting alloys: part 1—intermetallic phases," *Aluminium Transactions*, vol. 45, pp. 95–110, 2001.

[11] C. H. Caceres, C. J. Davidson, J. R. Griffiths, and Q. G. Wang, "The effect of Mg on the microstructure and mechanical behavior of Al-Si-Mg casting alloys," *Metallurgical and Materials Transactions A: Physical Metallurgy and Materials Science*, vol. 30, no. 10, pp. 2611–2618, 1999.

[12] F. H. Samuel, P. Ouellet, A. M. Samuel, and H. W. Doty, "Effect of Mg and Sr additions on the formation of intermetallics in Al-6 Wt% Si-3.5 Wt.% Cu-(0.45) to (0.8) Wt.% Fe 319-type alloys," *Metallurgical and Materials Transactions A*, vol. 29, no. 12, pp. 2871–2884, 1998.

[13] Q. G. Wang, "Microstructural effects on the tensile and fracture behavior of aluminum casting alloys A356/357," *Metallurgical and Materials Transactions A: Physical Metallurgy and Materials Science*, vol. 34, no. 12, pp. 2887–2899, 2003.

[14] S. S. Sreeja Kumari, R. M. Pillai, T. P. D. Rajan, and B. C. Pai, "Effects of individual and combined additions of Be, Mn, Ca and Sr on the solidification behaviour, structure and mechanical properties of Al–7Si–0.3Mg–0.8Fe alloy," *Materials Science and Engineering A*, vol. 460-461, pp. 561–573, 2007.

[15] E. A. Elsharkawi, E. Samuel, A. M. Samuel, and F. H. Samuel, "Effects of Mg, Fe, Be additions and solution heat treatment on the π-AlMgFeSi iron intermetallic phase in Al-7Si-Mg alloys," *Journal of Materials Science*, vol. 45, no. 6, pp. 1528–1539, 2010.

[16] L. Lu and A. K. Dahle, "Iron-rich intermetallic phases and their role in casting defect formation in hypoeutectic Al-Si alloys," *Metallurgical and Materials Transactions A: Physical Metallurgy and Materials Science*, vol. 36, no. 13, pp. 819–835, 2005.

[17] A. T. Joenoes and J. E. Gruzleski, "Magnesium effects on the microstructure of unmodified and modified Al-Si alloys," *Cast Metals*, vol. 4, no. 2, pp. 62–71, 1991.

[18] M. A. Moustafa, F. H. Samuel, H. W. Doty, and S. Valtierra, "Effect of Mg and Cu additions on the microstructural characteristics and tensile properties of Sr-modified Al-Si eutectic alloys," *International Journal of Cast Metals Research*, vol. 15, pp. 609–626, 2003.

[19] Y.-H. Tan, S.-L. Lee, and Y.-L. Lin, "Effects of Be and Fe additions on the microstructure and mechanical properties of A357.0 alloys," *Metallurgical and Materials Transactions A*, vol. 26, no. 5, pp. 1195–1205, 1995.

[20] S. Murali, K. S. Raman, and K. S. S. Murthy, "The formation of β-FeSiAl5 and BeFe phases in Al7Si0.3Mg alloy containing Be," *Materials Science and Engineering A*, vol. 190, no. 1-2, pp. 165–172, 1995.

[21] S. Murali, K. S. Raman, and K. S. S. Murthy, "Morphological studies on β-FeSiAl$_5$ phase in Al-7-Si-0.3Mg alloy with trace additions of Be, Mn, Cr, and Co," *Materials Characterization*, vol. 33, no. 2, pp. 99–112, 1994.

[22] S. Murali, A. Trivedi, K. S. Shamanna, and K. S. S. Murthy, "Effect of iron and combined iron and beryllium additions on the fracture toughness and microstructures of squeeze-cast Al-7Si-0.3Mg alloy," *Journal of Materials Engineering and Performance*, vol. 5, no. 4, pp. 462–468, 1996.

[23] L. Zhang, J. Gao, L. N. W. Damoah, and D. G. Robertson, "Removal of iron from aluminum: a review," *Mineral Processing and Extractive Metallurgy Review*, vol. 33, no. 2, pp. 99–157, 2012.

[24] Conservation of Mass in Chemical Changes Journal—Chemical Society, vol.64, part 2, Chemical Society, London, UK.

[25] F. H. Samuel, P. Ouellet, A. M. Samuel, and H. W. Doty, "Effect of Mg and Sr additions on the formation of intermetallics in AI-6 Wt Pet Si-3.5 Wt Pet Cu-(0.45) to (0.8) Wt Pet Fe 319-Type Alloys," *Metallurgical and Materials Transactions A: Physical Metallurgy and Materials Science*, vol. 29, no. 12, pp. 2871–2884, 1998.